IEEE Photonics Journal
An IEEE Photonics Society Publication

Open Access

Asynchronous Harmonic Mode Locking in an All-Normal Dispersion Yb-Doped Fiber Laser

Volume 5, Number 1, February 2013

Sheng-Min Wang
Siao-Shan Jyu
Wei-Wei Hsiang
Yinchieh Lai

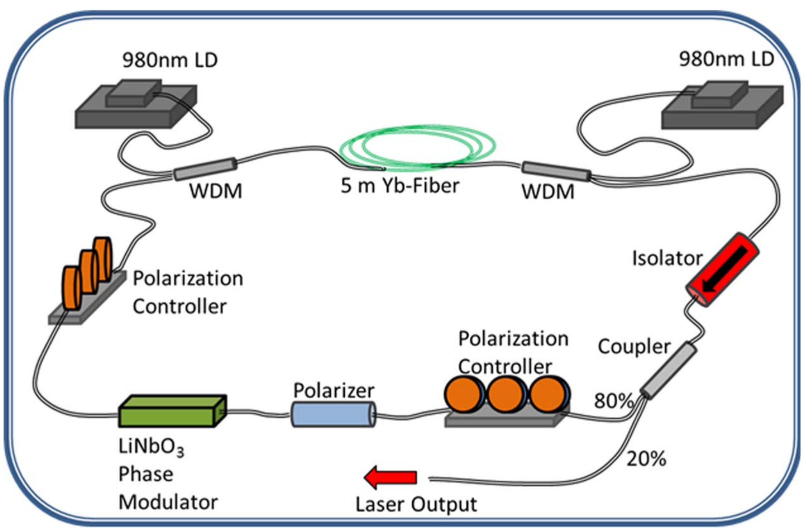

DOI: 10.1109/JPHOT.2013.2238916
1943-0655/$31.00 ©2013 IEEE

Asynchronous Harmonic Mode Locking in an All-Normal Dispersion Yb-Doped Fiber Laser

Sheng-Min Wang,[1] Siao-Shan Jyu,[1] Wei-Wei Hsiang,[2] and Yinchieh Lai[1]

[1]Department of Photonics and Institute of Electro-Optical Engineering, National Chiao-Tung University, Hsinchu 30010, Taiwan
[2]Department of Physics, Fu Jen Catholic University, Taipei 24205, Taiwan

DOI: 10.1109/JPHOT.2013.2238916
1943-0655/$31.00 ©2013 IEEE

Manuscript received October 24, 2012; revised January 4, 2013; accepted January 4, 2013. Date of publication January 11, 2013; date of current version February 4, 2013. This work was supported by the National Science Council of the under Contract NSC99-2221-E-009-045-MY3. Corresponding author: S.-M. Wang (e-mail: min.eo00g@nctu.edu.tw).

Abstract: We present detailed experimental and theoretical results to demonstrate the possibility of asynchronous harmonic mode locking in an all-normal dispersion fiber laser. In contrast to asynchronous soliton mode-locking operation in the anomalous dispersion regime, more profound laser dynamics are found. The experimentally demonstrated 10-GHz asynchronous harmonic mode-locked Yb-doped fiber laser exhibits an excellent super-mode noise suppression ratio in the RF spectrum with picosecond output pulsewidth.

Index Terms: Fiber lasers, mode-locked lasers.

1. Introduction

With the advances of fiber laser technologies, Yb-doped and Er-doped fiber lasers have become the widely used laser sources in the 1.0- and 1.5-μm wavelengths, respectively [1]. Many different types of CW, Q-switched, and mode-locked fiber laser configurations have been demonstrated on both types of the gain fibers. In particular, high-repetition-rate mode-locked Er-doped fiber lasers have been intensively developed due to their important applications on high-speed optical communication. Pulse repetition rates up to tens of gigahertz or more have been widely demonstrated by using various active harmonic mode-locking techniques [2], [3]. Within the same category of active mode locking, the asynchronous harmonic mode (AHM) locking approach [4], [5] is a particularly interesting one. Very stable laser operation with the 10-GHz-high repetition rate and subpicosecond pulsewidth has been demonstrated experimentally [6]–[9]. The AHM fiber laser exhibits many unique laser dynamics, which can be utilized for improving the laser stability and for achieving shorter pulsewidth [9]. The intracavity pulses are optical solitons, and their inherent stability allows them to overcome the perturbation effects of the intracavity phase modulation at a frequency slightly detuned from the cavity harmonic frequency by tens of kilohertz. The laser can be long-term stabilized by the economic deviation frequency locking technique, which only requires low-frequency electronics [7]. In contrast, high-repetition-rate active mode-locked Yb-doped fiber lasers are less investigated in the literature, even though there have been many studies on the passive mode-locked Yb-doped fiber lasers [10]–[12]. Phase-modulated harmonic mode locking [13] and regeneratively harmonic mode locking [14] are the two approaches that have been demonstrated successfully on Yb-doped fiber lasers operated up to the 10-GHz repetition frequency level. In view of the successes on Er-doped fiber lasers, it is natural for us to explore the

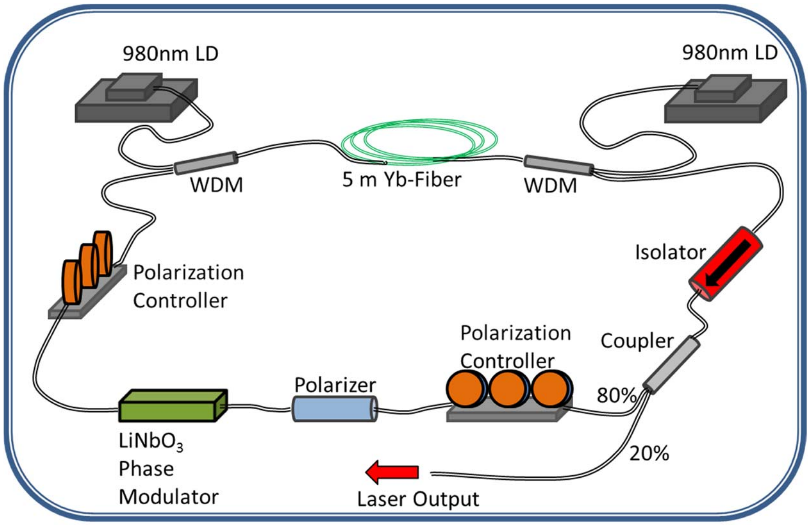

Fig. 1. Experimental setup of the AHM-locked Yb-doped fiber laser.

new possibility of asynchronous mode locking on Yb-doped fiber lasers [15]. In the present work, we will present detailed experimental and theoretical results to demonstrate that the asynchronous mode locking is another applicable technique for the high-repetition-rate Yb-doped fiber laser platform.

The fiber dispersion in the 1.0-μm wavelength regime is typically normal instead of anomalous as in the 1.5-μm wavelength regime. For the Yb-doped fiber lasers, one can choose to make the cavity average dispersion become anomalous through the use of dispersion compensation devices (i.e., chirped fiber gratings [10], grating pairs [13], and photonic crystal fibers [14]). Another approach is to work with the all-normal dispersion cavity [11]. Since the anomalous dispersion is required for optical solitons to form in the laser cavity, the intracavity pulses of an all-normal dispersion fiber laser will not be optical solitons as in the Er-doped fiber laser case. It will be very interesting to see whether the asynchronous mode-locking mechanism originally designed for soliton fiber lasers can still be effective under the new operation condition. Comparison of laser dynamics in the two operation states shall also shed us more new insights about the laser physics of asynchronous mode locking.

2. Experimental Demonstration

2.1. Laser Configuration

The experimental setup for our AHM Yb-doped fiber laser is illustrated in Fig. 1. Basically, it is an all-fiber hybrid mode-locked ring fiber laser configuration. The active mode-locking mechanism is through the use of a $LiNbO_3$ EO phase modulator, and the passive mode-locking mechanism is through the polarization additive pulse mode-locking technique [16]. The phase modulator is driven by the 10-GHz sinusoidal signal from an electronic synthesizer followed by a RF amplifier. Two semiconductor laser diodes near the 976-nm wavelength are used to bidirectionally pump the 5-m-long Yb-doped fiber (Nufern SM-YSF-LO) through the two wavelength-division multiplexing (WDM) couplers. The output coupler is with a 20/80 coupling ratio, and the inline isolator is to ensure single-directional lasing. Other fibers in the cavity are mainly the single mode fibers (Corning HI 1060) in the 1.0-μm wavelength. The total fiber length is about 23 m, and the fundamental cavity repetition frequency of the laser is 8.7 MHz. The laser is harmonic mode locked at 10 GHz (harmonic order $=$ 1150), and the typical output power is close to 20 mW under the total pump power around 180 mW.

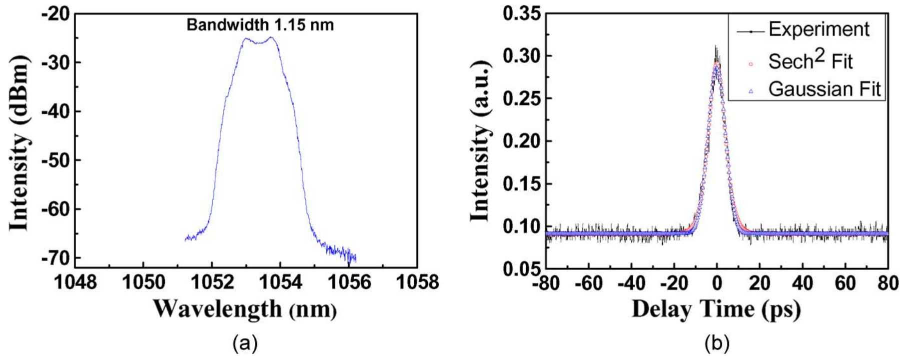

Fig. 2. (a) Optical spectrum and (b) autocorrelation trace of the output pulses.

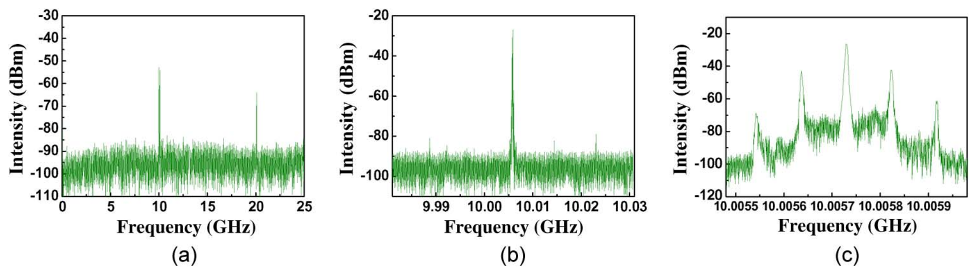

Fig. 3. (a) The 25-GHz, (b) 50-MHz, and (c) 500-kHz span of the RF spectra for the output pulse train.

2.2. Laser Characteristics

The studied Yb-doped fiber laser can be harmonic mode locked asynchronously or synchronously, depending on the adjustment of the modulation frequency. The output optical spectrum and the autocorrelation trace under AHM locking are shown in Fig. 2(a) and (b), respectively. The center wavelength is 1053.5 nm, and the 3-dB spectrum bandwidth is 1.15 nm. The pulsewidth is estimated to be 5.94 ps (Sech fitting) or 6.83 ps (Gaussian fitting). The corresponding fitting traces have also been plotted in Fig. 2(b). The time–bandwidth product is about 2.13 (Gaussian fitting), which indicates that the output pulse is chirped and the pulsewidth may be further reduced by a factor more than 4 with external chirp compensation.

Fig. 3 shows the RF spectra of the output pulse train in different spans. From the 25-GHz-span spectrum in Fig. 3(a), one can see that the Yb-doped fiber laser is harmonic mode locked very well at the 10-GHz repetition frequency even without any feedback control. The super-mode noise suppression ratio in the RF spectrum is better than 53 dB as can be seen in the 50-MHz-span spectrum in Fig. 3(b). It should be noted that the beating noises in the RF spectrum only indicate the existence of some super-modes. The measured ratio in RF spectral domain is related to, but not the actual intensity ratio of the super-modes in the optical frequency domain. In general, the relationship can be complicated since different super-mode noises can be even correlated [17]. In the studied laser, the suppression of super-modes should be mainly due to the gain competition mechanism. The combination effects of nonlinear self-phase modulation and optical bandpass filtering in the cavity may also help reduce the super-mode noises through pulse amplitude equalization. The RF spectral measurement results do indicate that the laser has achieved very good super-mode suppression when compared with typical harmonic mode-locked fiber lasers, even though the measured ratio is not the actual intensity ratio in the optical frequency domain. The asynchronous mode-locking characteristics can be clearly seen in the 500-kHz-span spectrum in Fig. 3(c). The deviation frequency is about 95 kHz. By also observing the output pulse train with a 20-GHz fast sampling oscilloscope, we did not see any indication of pulse drop. Therefore, the laser is well

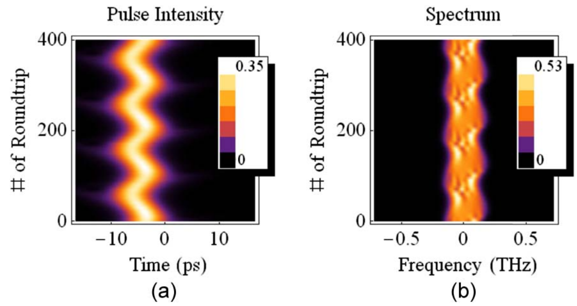

Fig. 4. Evolution plots for (a) pulse intensity and (b) frequency spectrum.

mode locked under the asynchronous mode-locking operation. From Fig. 3(c), one can also estimate the magnitude of the slow pulse timing oscillation amplitude Δt_0 according to the following equation [9]:

$$\Delta = \left| J_0[\omega_m \Delta t_0] / J_1[\omega_m \Delta t_0] \right|^2. \tag{1}$$

Here, Δ is the power ratio of the 0th- and 1st-order peaks in Fig. 3(c) while $\omega_m = 2\pi f_m$ is the modulation frequency. The obtained number for Δt_0 is around 4 ps. This value is in the same order of magnitude as in the Er-doped fiber laser case.

3. Theoretical Demonstration

3.1. Master Equation Model

The master equation model for asynchronous mode-locked lasers is given below [9]:

$$\frac{\partial u(T,t)}{\partial T} = \left(\frac{g_0}{1 + \frac{\int |u|^2 dt}{E_s}} - l_0 \right) u(T,t) + (d_r + jd_i) \frac{\partial^2}{\partial t^2} u(T,t) + (k_r + jk_i)|u(T,t)|^2 u(T,t) + jM \cos[\omega_m (t + RT)] u(T,t). \tag{2}$$

Here, the coefficients have the typical physical meanings: g_0 (linear gain), E_s (gain saturation energy), l_0 (linear loss), d_r (optical filtering), d_i (dispersion), k_r (equivalent fast saturable absorption), k_i (self-phase modulation), and T (evolution time in terms of the number of the cavity roundtrips). Since, experimentally, we did not use any optical filter in the laser cavity, here, the optical bandpass filtering effect represented by d_r will be due to the finite gain bandwidth. The last term is the asynchronous phase modulation term. Within this modulation term, $\omega_m = 2\pi f_m$ is the modulation frequency, and R is the linear timing walk-off per roundtrip due to the frequency offset of asynchronous mode locking. It is related to the offset frequency f_d by $R = N f_d / f_m^2$, with N being the harmonic mode-locking order. For an all-normal dispersion fiber laser, d_i and k_i will have different signs. In our notation, we choose to let $k_i > 0$ and thus $d_i < 0$ for the current studied laser.

3.2. Numerical Solution

The optical pulse shape in an all-normal dispersion mode-locked fiber laser is more complicated and may not be well approximated by the Gaussian or Sech pulse shape [18]. Therefore, we choose to directly solve the master equation numerically for studying the laser dynamics. The implicit Crank–Nichelson finite-difference method has been used as the numerical method. By choosing suitable parameters and initial conditions, we propagate the mater equation along the T-axis until the evolution of the solution becomes stable. One particular solution very similar to the experimental observation has been successfully found and is shown in Fig. 4. The time evolution of

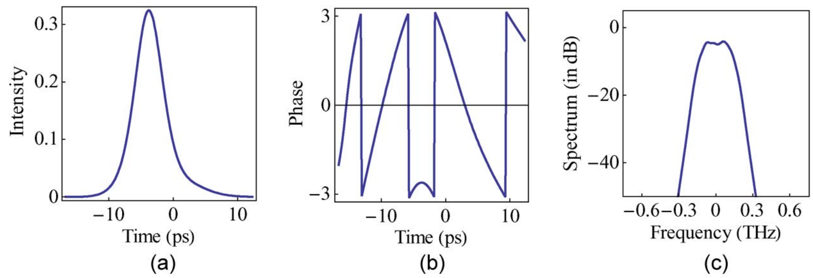

Fig. 5. (a) Pulse intensity, (b) pulse phase, and (c) time-averaged frequency spectrum.

the pulse intensity profile in Fig. 4(a) exhibits the slow timing oscillating behavior of asynchronous mode locking. More interestingly, the time evolution of the spectral profile in Fig. 4(b) exhibits new transient dynamics only seen in the normal dispersion regime. The spectral profile is flat top, and there are some small slow oscillating structures on the top of the spectra. There is also small slow oscillation of the center wavelength. The typical pulse intensity, phase, and the time-averaged spectrum are plotted in Fig. 5(a)–(c) for a better view. One can see that the pulse is with some chirps as expected. The distributions of real-time pulse intensity and phase are transiently asymmetric due to the slow oscillation. The numerically obtained pulsewidth, spectral bandwidth, and timing oscillation are of the same order with the experimental data. In particular, the calculated time-averaged spectral shape in Fig. 5(c) compares very well to the observed spectrum in Fig. 2(a), even though the real-time spectrum is transiently varying as shown in Fig. 4(b).

The normalized simulation parameters used to obtain the above solution are as follows: $d_i = -0.25$, $k_i = 1.0$, $d_r = 0.25$, $k_r = 0.3$, $l_0 = 0.8$, $g_0 = 4.0$, $E_s = 0.5$, $M = 0.5$, and $R = 1$. These parameters are chosen by the following procedure. We first choose the normalization time unit to be 1.0 ps so that the normalized pulsewidth will be with the order of magnitude 1. Under such time normalization, $d_r = -0.25$ will correspond to the net cavity dispersion $\beta_2 L = 0.5$ ps^2. The linear gain and loss are the typical values for similar fiber lasers. The gain saturation energy is chosen to let the normalized steady state pulse energy to be around 2, so that normalized pulse amplitude will also be with the order of magnitude 1. The value for R is estimated from the experimental 95-kHz deviation frequency. The value for M is the typical value for phase modulation. With all the above parameters fixed first based on the practical conditions, we then adjust the values for k_i, d_r, and k_r within the reasonable ranges to produce suitable pulse properties that can be compared to the experimental data. Through such careful consideration, we believe the set of parameters should be quite close to the actual situation of our laser.

From the numerical simulation, we have found that the laser dynamics of asynchronous mode locking are more profound in the normal dispersion regime. The self-silimar-like pulse shape and spectrum are certainly the common signatures of an all-normal dispersion mode-locked fiber lasers. However, the more interesting part is the transient oscillation behavior caused by asynchronous mode locking. The timing oscillation and center wavelength oscillation are already known from the soliton laser case, in which the pulse shape and the spectral shape are basically the same. The oscillating changes of the pulse shape and the spectral shape are more pronounced in the normal dispersion regime. This is mainly because the pulse is now chirped, and there is no soliton mechanism to maintain the pulse shape. The nonlinear pulse shortening effect through the polarization additive pulse mode-locking mechanism also plays an important role here. If we reduce the equivalent fast saturable absorption coefficient k_r to the smaller value of 0.2, the obtained solution plots are shown in Fig. 6. One can see that the oscillating changes of the pulse shape and spectral shape are now more severe. The average spectral shape also becomes non-flat top and narrower. We have also observed that the solutions in the normal dispersion regime are more sensitive to the equation parameters.

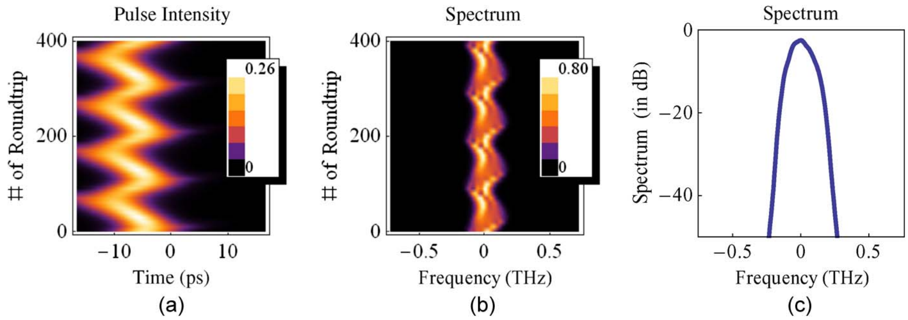

Fig. 6. (a) Pulse intensity, (b) spectrum, and (c) time-averaged spectrum with a smaller k_r.

4. Conclusion

To conclude, we have investigated both experimentally and theoretically to demonstrate the possibility of AHM locking in an all-normal dispersion fiber laser. A Yb-doped fiber laser has been successfully AHM locked at 10 GHz with picosecond pulsewidth. The fiber cavity is with all-normal dispersion, and thus, the optical pulses circulated inside the cavity are not solitons. Nevertheless, very good super-mode suppression capability of asynchronous mode locking in the normal dispersion regime has been experimentally confirmed. This should open up many new possibilities for extending the asynchronous mode-locking techniques to different types of fiber lasers. In contrast to asynchronous soliton mode-locking operation in the anomalous dispersion regime, more profound transient laser dynamics have also been theoretically found. In particular, slow oscillation of the pulse shape and the spectral shape is more pronounced due to the lack of soliton effects. The laser operation is also more sensitive to the nonlinear pulse shortening effects. Currently, the experimental pulsewidth is mainly limited by the available intracavity nonlinearity and can be further improved in the future.

References

[1] M. E. Fermann and I. Hartl, “Ultrafast fiber laser technology,” *IEEE J. Sel. Topics Quantum Electron.*, vol. 15, no. 1, pp. 191–206, Jan. 2009.
[2] B. Bakhski and P. A. Andrekson, “40 GHz actively modelocked polarisation-maintaining erbium fibre ring laser,” *Electron. Lett.*, vol. 36, no. 5, pp. 411–413, Mar. 2000.
[3] M. Nakazawa and E. Yoshida, “A 40-GHz 850-fs regeneratively FM mode-locked polarization-maintaining erbium fiber ring laser,” *IEEE Photon. Technol. Lett.*, vol. 12, no. 12, pp. 1613–1615, Dec. 2000.
[4] C. R. Doerr, H. A. Haus, and E. P. Ippen, “Asynchronous soliton mode-locking,” *Opt. Lett.*, vol. 19, no. 23, pp. 1958–1960, Dec. 1994.
[5] H. A. Haus, D. J. Jones, E. P. Ippen, and W. S. Wong, “Theory of soliton stability in asynchronous modelocking,” *J. Lightw. Technol.*, vol. 14, no. 4, pp. 622–627, Apr. 1996.
[6] W. W. Hsiang, C. Y. Lin, M. F. Tien, and Y. C. Lai, “Direct generation of a 10 GHz 816 fs pulse train from an erbium-fiber soliton laser with asynchronous phase modulation,” *Opt. Lett.*, vol. 30, no. 18, pp. 2493–2495, Sep. 2005.
[7] W. W. Hsiang, C. Y. Lin, N. K. Sooi, and Y. C. Lai, “Long-term stabilization of a 10 GHz 0.8 ps asynchronously mode-locked Er-fiber soliton laser by deviation-frequency locking,” *Opt. Exp.*, vol. 14, no. 5, pp. 1822–1828, Mar. 2006.
[8] E. S. Boncristiano, L. A. M. Saito, and E. A. De Souza, “396 fs pulse from an asynchronous mode-locked erbium fiber laser with 2.5–12 GHz repetition rate,” *Microw. Opt. Technol. Lett.*, vol. 50, no. 11, pp. 2994–2996, Nov. 2008.
[9] W. W. Hsiang, H. C. Chang, and Y. Lai, “Laser dynamics of a 10 GHz 0.55 ps asynchronously harmonic modelocked Er-doped fiber soliton laser,” *IEEE J. Quantum Electron.*, vol. 46, no. 3, pp. 292–299, Mar. 2010.
[10] B. Ortac, M. Plotner, T. Schreiber, J. Limpert, and A. Tunnermann, “Experimental and numerical study of pulse dynamics in positive net-cavity dispersion mode-locked Yb-doped fiber lasers,” *Opt. Exp.*, vol. 15, no. 23, pp. 15 595–15 602, Nov. 2007.
[11] A. Chong, W. H. Renninger, and F. W. Wise, “Environmentally stable all-normal-dispersion femtosecond fiber laser,” *Opt. Lett.*, vol. 33, no. 10, pp. 1071–1073, May 2008.
[12] S. A. Zhou, D. G. Ouzounov, and F. W. Wise, “Passive harmonic mode-locking of a soliton Yb fiber laser at repetition rates to 1.5 GHz,” *Opt. Lett.*, vol. 31, no. 8, pp. 1041–1043, Apr. 2006.
[13] N. G. Usechak, G. P. Agrawal, and J. D. Zuegel, “Tunable, high-repetition-rate, harmonically mode-locked ytterbium fiber laser,” *Opt. Lett.*, vol. 29, no. 12, pp. 1360–1362, Jun. 2004.

[14] K. Koizumi, M. Yoshida, T. Hirooka, and M. Nakazawa, "10 GHz, 1.1 ps optical pulse generation from a regeneratively mode-locked Yb fiber laser in the 1.1 mu m band," *Opt. Exp.*, vol. 19, no. 25, pp. 25 426–25 432, Dec. 2011.
[15] S. M. Wang, S. S. Jyu, W. W. Hsiang, and Y. Lai, "Demonstration of 10 GHz asynchronous mode-locking on a ytterbium-doped fiber laser with normal dispersion," in *Proc. CLEO-PR*, Sydney, Australia, Aug. 2011, p. C221.
[16] H. A. Haus, "Mode-locking of lasers," *IEEE J. Sel. Topics Quantum Electron.*, vol. 6, no. 6, pp. 1173–1185, Nov./Dec. 2000.
[17] S. Gee, F. Quinlan, S. Ozharar, and P. J. Delfyett, "Correlation of supermode noise of harmonically mode-locked lasers," *J. Opt. Soc. Amer. B, Opt. Phys.*, vol. 24, no. 7, pp. 1490–1497, Jul. 2007.
[18] F. O. Ilday, J. R. Buckley, W. G. Clark, and F. W. Wise, "Self-similar evolution of parabolic pulses in a laser," *Phys. Rev. Lett.*, vol. 92, no. 21, pp. 213902-1–213902-4, May 2004.